Article

Author for correspondence:
Ian M. Howat, E-mail: ihowat@gmail.com

Temporal variability in snow accumulation and density at Summit Camp, Greenland ice sheet

Ian M. Howat

Byrd Polar and Climate Research Center & School of Earth Sciences, The Ohio State University, Columbus, USA

Abstract

A 3-year record of weekly snow water equivalent (SWE) accumulation at Summit Camp, central Greenland ice sheet, obtained by direct sampling, is presented. While the overall SWE accumulation of 24.2 cm w.e. a^{-1} matches long-term ice core estimates, variability increases at shorter timescales. Half of the annual SWE accumulation occurs during a few large events, with the average accumulation rate decreasing 35% between the first and second halves of the record coinciding with exceptional anticyclonic conditions in the spring and summer of 2019. No seasonality in accumulation is detected. Rather, local accumulation rates appear to be significantly impacted by wind redistribution that obscures temporal patterns in snowfall. Surface snow density is consistent, on average, with previously measured values but does not correlate with near surface temperature or wind speed. Two surface mass balance reanalysis models significantly underestimate accumulation rates at Summit Camp. This is concerning because such models are often used to estimate ice-sheet mass loss.

1. Introduction

The surface mass balance (SMB) of the Greenland ice sheet is, primarily, the difference between the mass gained through snowfall and that lost due to melt runoff (Lenaerts and others, 2019). Greenland's annual SMB has declined over the past three decades due to increased melting relative to snowfall. The rates of iceberg calving and melting at the ice/ocean interface have also increased, resulting in an increasingly negative total mass balance and an increasing contribution to sea level rise (IMBIE Team, 2020). Snowfall accumulation is the single largest term in the Greenland ice-sheet mass budget and has the largest interannual variability (Box and others, 2013; Gallagher and others, 2022). Accumulation is also highly complex since it is dependent on both large-scale atmospheric circulation and local-scale surface processes, including wind redistribution. The characteristics of accumulated snow also change quickly through time by multiple metamorphic processes that are also dependent on atmospheric conditions. Understanding and predicting accumulation, therefore, requires detailed observations of snow and firn at a wide range of spatial and temporal scales (Lenaerts and others, 2019).

Much of our understanding of the mass of snow accumulation on ice sheets comes from relatively sparse measurements from ice cores, snow pits or inferences based on remotely sensed data. These are limited to, typically, annual resolution or, in the case of remotely sensed data, subject to significant uncertainties regarding snow density, grain size or other physical properties required to estimate mass accumulation (McIlhattan and others, 2020). No direct measurements of mass accumulation and near-surface density on ice sheets at higher temporal resolution over multiple years are known to exist. This is because of the logistical challenges of obtaining field measurements. There is, therefore, a critical gap in direct observations of mass accumulation and surface density at the temporal scale of atmospheric and surface variability which are necessary for process understanding. Furthermore, such measurements provide valuable ground truth for remote sensing. For example, the success of satellite-altimetry missions, such as ICESat-2, is dependent on the ability to obtain estimates of ice-sheet mass balance from changes in surface elevation, thus requiring knowledge of the density of the accumulation and the changes in firn density that contribute to surface height changes. Additionally, atmospheric reanalysis models, another primary source for ice-sheet mass-balance estimates and forcing for firn models used to correct altimetry measurements (e.g. Kuipers Munneke and others, 2015), rely on ground measurements for calibration and validation. As such, the ability of these models for representing accumulation is not well constrained (Fettweis and others, 2020; Montgomery and others, 2020). Due to the vastness of ice-sheet interiors, small biases in the rate of surface accumulation can cause large errors in mass balance. For example, a 1 cm a^{-1} bias in the rate of annual water-equivalent accumulation over the Greenland ice sheet equates to 15 Gt a^{-1} of mass, or over 5% of the current rate of loss (IMBIE, 2020).

Located at the highest point of the interior Greenland ice sheet and occupied year-round for over 20 years, Summit Camp provides a unique platform for supporting observational campaigns that require frequent and sustained manual measurements, equipment maintenance and sheltered laboratory facilities. These include detailed measurements of a wide range of atmospheric variables (e.g. Box and Steffen, 2001; Castellani and others, 2015; Berkelhammer and others, 2016), snow accumulation (e.g. Dibb and Fahnestock, 2004) and
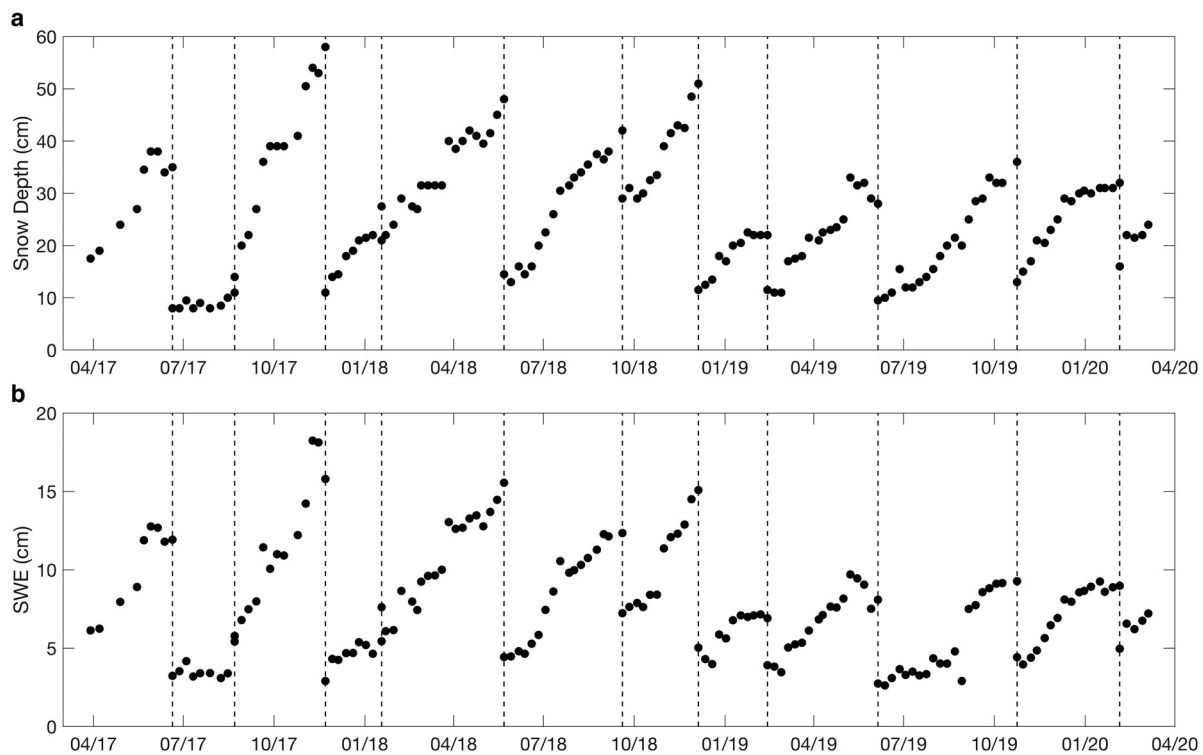
Fig. 1. Time series of snow board (A) sample snow depth, as measured from the surface to the board, and (B) sample SWE thickness, obtained from average of sample mass and volume measurements. Dashes denote transitions in sampling sites.

firn density (e.g. Zwally and Li, 2002). As a result, much of our understanding of large-scale processes and atmospheric drivers controlling Greenland's accumulation comes from observations at Summit Camp. Yet, a sustained program of measuring mass accumulation and surface density through time had not been undertaken.

To fill this observational gap and provide a benchmark dataset for instrument calibration and validation, measurements of changes in the mass and thickness of surface accumulation were obtained manually at ~7-d intervals for 3 years at Summit Camp. These measurements provide unprecedented information about temporal variability in surface mass accumulation and surface snow density.

While a preliminary version of the first year of these observations was shown in Howat and others (2018), the full 3-year dataset is presented here, including quality control and errors. The observations are then used to examine temporal variability in snow water equivalent (SWE) accumulation and density at various timescales and in relation to local meteorology. Finally, the mass accumulation estimates are compared to concurrent measurements of snow height change at a network of stakes, snowfall observed by ground-based Doppler radar and accumulation rates predicted by two ice-sheet SMB reanalysis models often used for estimating ice-sheet mass changes.

2. Snow board measurements

Observations of accumulation thickness, SWE thickness and density were obtained using the snow board method, where accumulation atop a board, which serves as a depth reference, is repeatedly sampled and measured. The snow board method has been used for over a century to measure mountain snowpack (e.g. Wayand and others, 2015), but no application to measuring ice-sheet accumulation was found in the literature. A shallow, rectangular pit is excavated, and a piece of plywood is placed over the floor of the pit. The pit is then allowed to fill with snow and settle over a period of at least 2 weeks. A plastic tube

is used to remove a core sample of the snow from the surface to the plywood, which serves as a depth reference for each subsequent sample. The sample is taken from a different location on the board each time, as measured from flagged poles at the corner of the plywood, to provide an undisturbed sample. The SWE of the sample is obtained from both its mass and water volume, providing redundancy for quality control. To obtain the SWE thickness of the sample from its mass, the sample is brought indoors in its sampling tube and weighed. The weight of the empty sampling tube is subtracted, and this weight is divided by the cross-sectional area of the tube. To obtain the SWE thickness from the sample volume, the sample is allowed to melt and the liquid volume is divided by the cross-sectional area of the core. The snow depth at each sampling site is also recorded. The SWE estimate divided by this depth gives an estimate of sample density. Measurement precisions and resulting uncertainties are provided in the Supplementary material.

When no undisturbed locations remain on the board, or the snow becomes too deep to sample, sampling moves to a new, adjacent snow board site. During the change to a new site, samples are taken at the same time at both the old and new sites. These are termed tie points. Subtracting the SWE value of the tie point at the new site from that of the old site, and adding this difference to later measurements, gives the cumulative change in SWE across site transitions. The snow board sampling sites were in a designated area of undisturbed snow, upwind of other field instrumentation and buildings to minimize their influence on accumulation.

A total of 147 measurements were recorded between 7 March 2017 and 5 March 2020, averaging 7 ± 2 d between surveys (Fig. 1). Measurements of snow depth ranged from 8 to 58 cm, with a mean of 26.7 ± 11.9 cm. Survey sites were occupied 90 d, on average, with the longest being 141 d from 5 June to 24 October 2019. The shortest, 29 d, was the final site.

SWE observations obtained from sample mass ranged from 2.62 to 18.40 cm w.e., averaging 8.00 cm w.e. and with a std dev.

of ±3.43 cm w.e. On average, SWE derived from mass was 0.05 cm w.e., or 0.75%, less than that derived from volume, with the RMS of differences equaling 0.15 cm w.e. (note this was mistakenly reported as 1.5 cm w.e. in Howat and others, 2018), or 1.9% and with 95% of measurements within 0.31 cm w.e. or 3.2% (Fig. S1). The disagreement between mass and volume measurements tends to increase with sample size, with a std dev. of 0.11 cm w.e. below 10 cm w.e. and 0.21 cm w.e. above, and no measurements agree within 0.2 cm w.e. for samples over 14 cm w.e. This indicates some unknown instrumental or procedural error in larger samples, and it is not known whether this impacts mass, volume or both measurements. A description of dataset quality control is provided in the Supplementary material.

3. Results

Subtracting differences between concurrent tie-point measurements at sample site transitions provides an estimate of the cumulative SWE thickness over the 3-year record (Fig. 2a). Total SWE accumulation was 69.5 ± 0.2 cm w.e. for an average rate of 24.2 cm w.e. a^{-1}, equal within uncertainty to the long-term annual rate of 24 cm w.e. obtained from the GISP ice core (Alley and others, 1993). Subtracting this average trend from the time series (Fig. 2b), there is no clear seasonality. Instead, the time series is dominated by multi-year variability punctuated by distinct periods of increasing and decreasing accumulation. Following a sustained period of declining SWE between May and August 2017, the rate of accumulation was approximately one-third greater than the mean between October 2017 and January 2019. The accumulation rate then declined to two-thirds of the mean from January 2019 through the rest of the record. Overall, the accumulation rate of 28.6 cm a^{-1} during the first half of the record was 35% greater than the 18.6 cm a^{-1} during the second half. This interannual variability appears to be a consequence of more frequent, large accumulation events in 2017 and 2018. Out of the six measurements of increased accumulation >3 cm w.e. per 7 d, five occur before April 2018, with the sixth in October 2018 (Fig. 2c). These large increases are typically followed by rapid declines of 1–2 cm w.e. over the following one to three measurements. However, two significant 7-d declines of 1.5 and 1 cm w.e. occurred on 22 May 2019 and 16 January 2020, respectively, that were not preceded by accumulation events.

One-quarter of the observations recorded a decrease in SWE from the previous measurement. The 10th and 90th percentiles of the 7-d change in SWE were −0.36 and 1.60 cm, respectively, with a maximum gain of 4.01 cm, or one-sixth the annual accumulation, between 2 and 9 November 2017, followed closely by the maximum observed loss of 2.33 cm between 15 and 22 November 2017. Increases greater than the 90th percentile accounted for 50% of the total cumulative SWE. Over the record, declines in SWE totaled 16.60 cm, or 24% of the cumulative total, with half of that loss occurring in the first year when overall accumulation rates were larger.

Density obtained by dividing sample SWE by snow depth ranged from 0.201 to 0.441 g cm^{-3} with a mean of 0.303 g cm^{-3} and a std dev. of ±0.044 g cm^{-3} (Fig. 2d). This is nearly identical to the average of 0.305 g cm^{-3} measured by Dibb and Fahnestock (2004) for the upper 1 m at Summit Camp, and slightly less than the average of 0.315 g cm^{-3} for 10 cm depth from 200 measurements from across Greenland (Fausto and others, 2018). The time series of density shows three sharp minima in January 2018, October 2018 and August 2018, with less defined maxima between. The highest densities, reaching over 0.4 g cm^{-3} occur at the transfer from the first to second snow board site in July 2017, which were measured from samples with thicknesses <10 cm. Density then decreased to the January 2018 minimum of 0.21 g cm^{-3}.

The lowest recorded density of 0.20 g cm^{-3} on 15 August 2019 was observed during a period of high variability. Overall, density declined by −0.022 g cm^{-3} a^{-1}. However, excluding the period of anomalously high densities and lower sample depths before 15 August 2017, the trend declines by nearly half, to −0.012 g cm^{-3} a^{-1}.

Interpretation of the density record recovered from the snow board samples is complicated by the varying sample depth. Density should vary, in part, as a function of sample snow depth as deeper samples will tend to include older snow that has undergone more metamorphism. Conversely, as mentioned above, thinner samples may include a larger fraction of wind-packed surface layers of high density. However, the plot of density and snow depth (Fig. 3) shows no consistent relationship. As shown previously, densities are highest for the thinnest snow depths measured between 20 June and 22 August 2017. Other periods with nearly as thin snow depths, however, do no not have anomalously high densities, indicating that the anomaly was specific for that time period. The most variability in density occurs for snow depths between 18 and 22 cm. While maximum densities remain consistent at ~0.350 g cm^{-3} across snow depths above 10 cm, minimum densities decline to below 0.24 g cm^{-3} within this depth range.

This high variability in sample density indicates an inconsistent relationship between changes in snow depth and changes in SWE. Changes in SWE between measurements are plotted against changes in snow depth in Figure 4. Three outliers with values >3 std dev. from the best fit line occur in September and November 2017. The November 2017 outliers occur when snow depths are the highest recorded, at over 50 cm. As described in Section 2, samples from the largest snow depths may have larger errors. The 27 September 2017 outlier occurred earlier at the sampling site during a period of rapid accumulation, but it is unclear if this measurement is erroneous. Removing these outliers, changes in snow thickness correspond to 61% of the variability in SWE with an average density equivalent of 0.278 g cm^{-3}. Using this density, predicting changes in SWE from changes in sample thickness would give an RMS error of 0.52 cm w.e., or 106% the average change in SWE between 7-d observations. However, the fractional error in SWE estimated from snow thickness change tends to decrease with time. After 1 year, the cumulative thickness scaled by the average density (0.278 g cm^{-3}) is 1.70 cm w.e., or <6% of the observed 29.49 cm w.e. This fractional difference remains near 5% for the remainder of the record. Therefore, if a long-term mean surface density can be established and compaction can be accounted for, this suggests that SWE may be estimated from changes in accumulation thickness to a precision comparable to the snow board measurement precision (e.g. ±3%). This estimate may be improved through statistical modeling, such as applied to seasonal snow by Sturm and others (2010).

4. Comparison to meteorological observations

Meteorological variables including air temperature 2 m above the surface, wind speed, wind direction and barometric pressure have been recorded by the U.S. National Oceanic and Atmospheric Administration (NOAA) at an automatic weather station at Summit Camp nearly continuously since 2008. Hourly data were obtained from the NOAA Earth System Research Laboratory Global Monitoring Division data portal (https://gml.noaa.gov/aftp/data/meteorology/in-situ/sum/, last accessed: 21 November 2021). Daily and 30-d retrospective means are compared to the snow board observations of detrended cumulative SWE accumulation and density in Figures S2 and S3 in the Supplementary material.
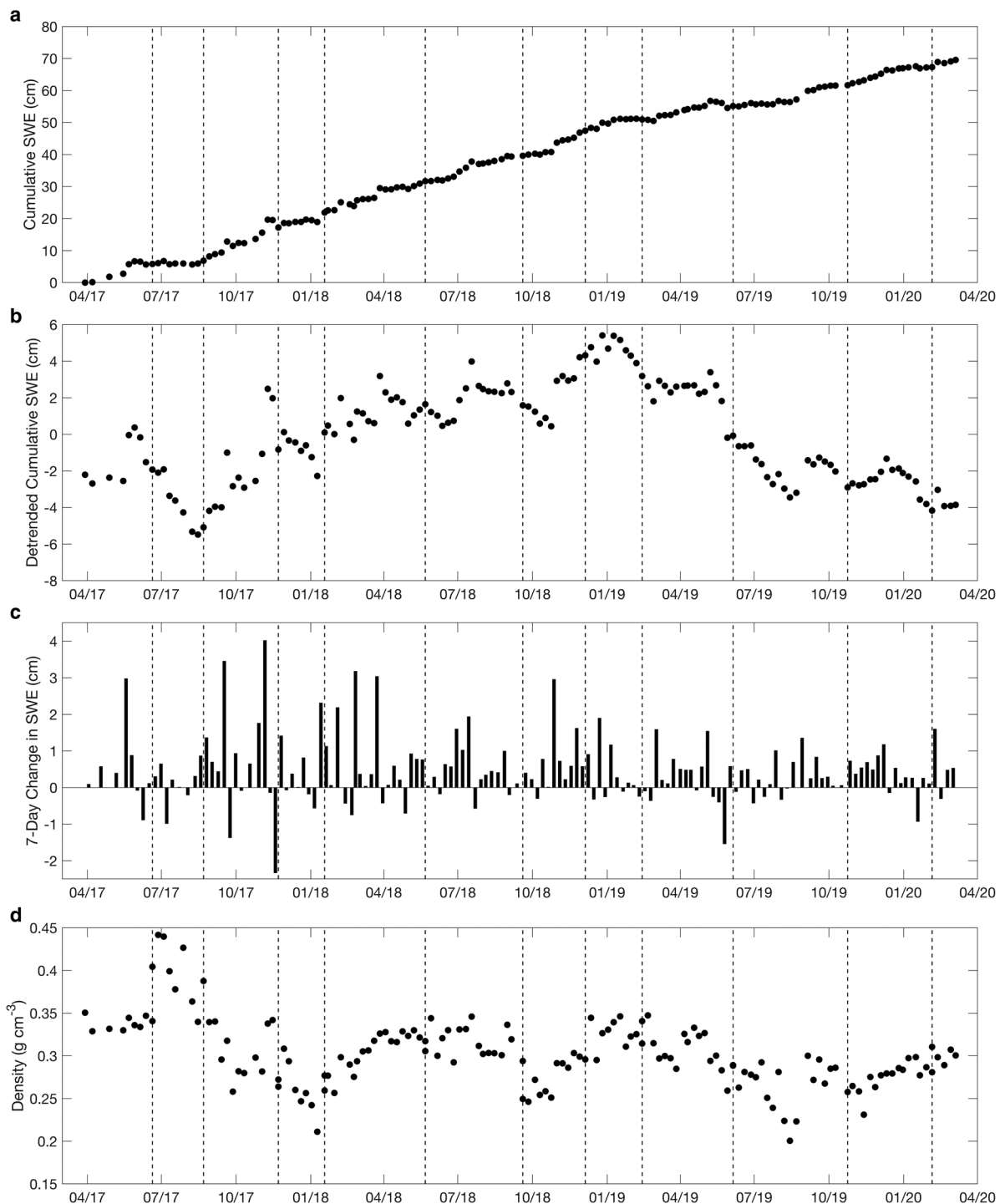
Fig. 2. (A) Cumulative SWE thickness obtained from differencing concurrent measurements between sample sites (i.e. tie-point measurements). (B) Same as in (A) but with a rate of 24 cm w.e. a^{-1} subtracted. (C) Seven-day change in SWE between measurements. Dashes denote changes in sampling board sites. (D) Sample density obtained by dividing SWE by the snow depth.

The decrease in accumulation rate between April and August 2019 corresponds with sustained high pressure, with a 30-d retrospective average value reaching 687 hPa. This value is greater than the 99th percentile over the 2008–2021 meteorological record and was a major ablation event throughout Greenland (Tedesco and Fettweis, 2020). The largest decrease in SWE (−1.6 cm w.e.) between observations occurred between 22 and 28 May 2019, when daily average pressure reached near 700 hPa. It is unclear what caused this decrease, as wind speeds were depressed to below 5 m s^{-1} and temperatures were −10°C or less. This rate of decreasing SWE is far greater than could be attributed to sublimation (Box and Steffen, 2001).

The highest wind speeds observed since 2008 occurred in January and February 2018, with a 30-d average reaching 11 m s^{-1} and a peak speed of 21.7 m s^{-1} on 23 February 2018. Another period of high winds occurred at the end of the record, with a 30-d mean reaching 9.3 m s^{-1} on 1 February 2020. Neither of these periods of anomalous winds corresponded with anomalies in SWE accumulation. Overall, mean wind speed between snow board observations explains only ~5% of the variability in accumulation. Additionally, there is no apparent correlation between accumulation and wind direction, as previously detected for snowfall (Castellani and others, 2015).

Density is expected to vary with air temperature and pressure, which closely track each other at Summit Camp, through crystal
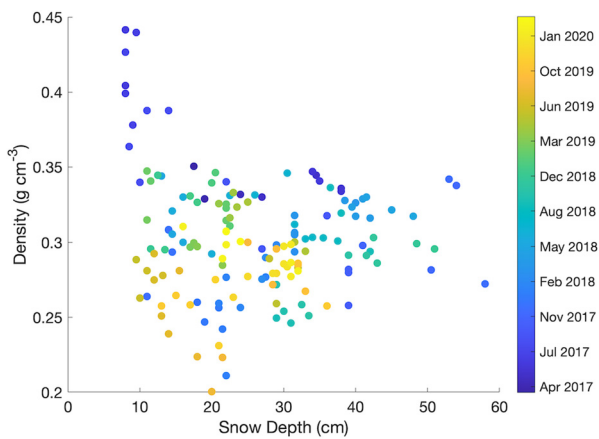
Fig. 3. Comparison of snow sample depth to density. Color scale is sample observation date.
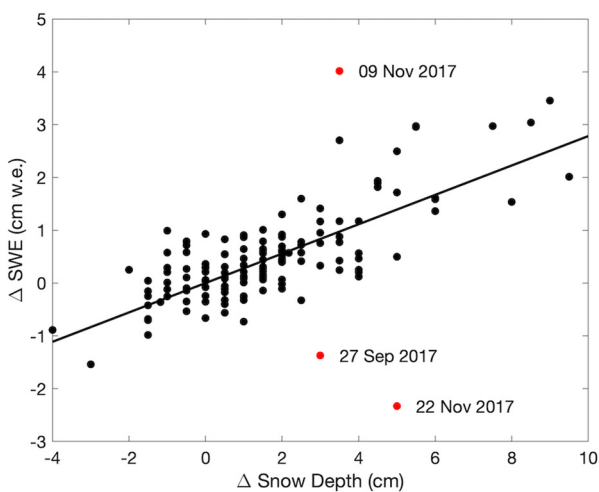
Fig. 4. Change in snow depth versus change in SWE between observations. Outliers are marked in red with observation dates. The precision of snow depth measurements is 0.5 cm. Black curve is the best fit line, corresponding to a density of 0.278 g cm^{-3}.

grain growth in the atmosphere and rates of dry snow metamorphism in the snowpack (e.g. Zwally and Li, 2002; Fausto and others, 2018). Wind should also play a role in controlling turbulent heat and vapor fluxes at the surface. Comparing the density record to daily averaged surface air temperature and wind speed, however, reveals no consistent relationship (Fig. S3). Over the first 18 months, density tracks air temperature and pressure, falling from the highest observed values between 20 June and 22 August 2017, to a minimum in January 2018, and then rising and falling with temperature and pressure through October 2018. After this period, however, variations in density decouple from air temperature and pressure, showing little or no seasonal cycle. Conversely, density does not appear to track wind speed in the first half of the record, with highs in density occurring, generally, during periods of lower wind speed. After October 2018, however, density appears to vary with wind speed, declining during a period of lower wind speeds during summer 2019, and then increasing in tandem at the end of the record. Variations in density vary weakly ($r^2 = 0.06$) but significantly ($p = 0.005$) with the 30-d mean wind direction, increasing in density as winds move from the southeast (130°) to southwest (210°). A possible explanation for this correlation may be snowfall type. Pettersen and others (2018) found that southeasterly winds correspond with precipitation from ice clouds, whereas southwesterly winds correspond with snowfall from warmer, mixed-phase clouds.

5. Comparison to the 'bamboo forest' snow stake network

As with any point measurement, it is uncertain how representative the snow thickness measurements at the snow board sampling sites are to the greater Summit Camp region. Variations in surface height have been measured at a network of snow stakes, nicknamed 'the bamboo forest', at Summit Camp continuously since 2003. As with the snow board snow thickness measurements, these stakes record changes in surface accumulation and ablation, but also record compaction between the surface and the base of the stakes (Dibb and Fahnestock, 2004). Therefore, if the changes in snow thickness are equivalent between the snow board site and the bamboo forest, they should display the same short-term variations, but increasingly diverge by amount equal to the increased compaction rate at the stakes relative to the snow board.

Snow stake data are obtained from the Summit Camp data repository (https://conus.summitcamp.org, last accessed: 21 November 2021). The cumulative stake height change is obtained from the average change of individual stake measurements. The cumulative change in snow depth of the snow board samples is plotted with cumulative change in stake height in Figure 5. While the two records have similar short-term variations, they increasingly diverge, with the snowboard measurements becoming increasingly greater than the snow stake measurements at an average rate of 15.12 cm a^{-1}. Such a trend is expected as the snow stakes record both the amount of accumulation and the surface lowering due to densification between the surface and the base of the stakes (Dibb and Fahnestock, 2004). A compaction rate of 15.12 cm a^{-1} is consistent with field measurements and modeling (Dibb and Fahnestock, 2004). Adjusting the snow stake record for compaction by adding the trend of 15.12 cm a^{-1} results in a close match with the snow board record (Fig. 5b), yielding an RMS of differences of 4.0 cm, well within the snow stake std dev. of 8.2 cm. As expected, the average of the snow stake measurements has a smaller magnitude of short-term variability than the point measurement provided by the snow board. Notably, the short-term minima in snow depth change averaged from the snow stakes on 10 August 2017 and 28 July 2019 were 6.0 and 4.0 cm less, respectively, than the snow board. Additionally, several short-term peaks in snow depth change are visible in the snow board record that are not reflected in the snow stake average, particularly a sustained increase of up to 7.4 cm between October 2018 and February 2019. Thus, this comparison suggests that the snow board measurements are broadly representative of the larger Summit Camp area, when additionally accounting for snow compaction. Short-term (monthly or less) variability, however, may reflect local conditions within the range expected from the individual snow stake measurements.

6. Comparison to the precipitation occurrence sensor system

SWE accumulation reflects variations in both snowfall and wind redistribution. To separate these contributions, the snow board accumulation record is compared to snowfall measured by the precipitation occurrence sensor system (POSS). The POSS is a continuous wave, X-band Doppler radar deployed at Summit Camp as part of the Integrated Characterization of Energy, Clouds, Atmospheric state and Precipitation at Summit (ICECAPS) project (Sheppard and Joe, 2008; Castellani and others, 2015). The POSS samples ~1 m^3 of air directly above the transmitter and receiver, providing observations of near-surface precipitation type, amount and frequency, in liquid w.e. Hourly snowfall rates are obtained from NOAA Physical
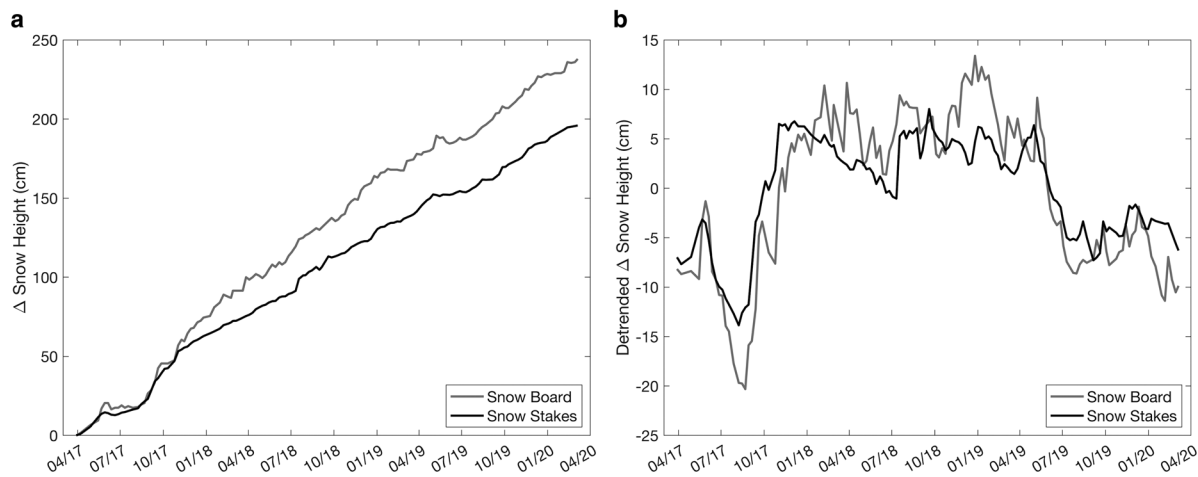
Fig. 5. (A) Cumulative change in (black) surface height measured at the snow stake network and (gray) snow board sample thickness. (B) Same as (A) with the best fit linear trend removed.

Sciences Laboratory (ftp://ftp1.esrl.noaa.gov/psd3/arctic/summit/poss/processed/, last accessed: 21 November 2021).

The instantaneous w.e. snowfall rates measured by the POSS are converted into cumulative SWE to compare to the snow board SWE record (Fig. 6a). We note that because the POSS only records snowfall, and not ablation, we would expect it to estimate a greater accumulation than the snow board. Cumulative POSS snowfall, however, is 21.2 cm w.e. over the 3-year period, or less than a third of the 69.5 cm w.e. measured from the snow board, remaining between 26 and 33% of the snow board measurement after the first year. Castellani and others (2015) suggested that underestimation of accumulation by the POSS, compared to the snow stake network in that case, may be mostly due to biases in the calibration used for converting reflectivity to the snowfall.

Subtracting the trend from each time series (Fig. 6b), there is little or no agreement in sub-annual variability. Consistent with Bennartz and others (2019), the POSS shows seasonal peaks in snowfall rate in August and September of 2017 and 2018. However, no such peak is visible in 2019, which was the summer of persistent anticyclonic conditions over central Greenland (Tedesco and Fettweis, 2020).

At the timescale of individual observations, there is a weak ($r^2 = 0.08$) but significant ($p = 10^{-3}$) correlation between changes in POSS cumulative snowfall and changes in snowboard cumulative SWE (Fig. 6c). No loss in SWE between snowboard observations occurred when the change in cumulative snowfall was >4 mm w.e., with all losses >1 cm occurring when cumulative snowfall was near zero. Large increases in SWE at the snow board, however, do not appear correlated with cumulative snowfall, with anomalously large (>2 cm w.e.) increases in SWE occurring with cumulative snowfalls of 3 mm w.e. or less.

## 7. Comparison to atmospheric reanalysis model estimates

Atmospheric reanalysis models are widely used to provide estimates of surface accumulation and ice-sheet mass balance. The snow board measurements provide a rare opportunity to validate model estimates for changes in SWE, which is equivalent to SMB on ice sheets, at high temporal resolution over multiple years. The snow board SWE measurements are compared to two regional reanalysis models with openly available output for ice-sheet accumulation: the Modern Era Retrospective analysis for Research and Applications version 2 (MERRA-2) (Gelaro and others, 2017) and the Modèle Atmosphérique Régional (MAR) (Fettweis and others, 2013).

MERRA-2 Land Ice Surface Diagnostics estimates are provided by NASA Global Modeling and Assimilation Office (GMAO) using the Goddard Earth Observing System Model (GEOS) version 5.12.4 (GMAO, 2015). MERRA-2 contains a snow process model that tracks surface mass and heat fluxes (Cullather and others, 2014). The model output, posted at 0.5° × 0.625° resolution, includes 3-hourly estimates of the total mass of the snow and firn layer, which are differenced to provide the SMB in w.e. thickness. The time series of cumulative SWE at the snow board location is obtained through bilinear interpolation of the 3-hourly grids to the snow board coordinates. Since the time of the snow board observation was not recorded, we compare cumulative MERRA-2 SWE values obtained at noon UTC of each day to the snowboard measurements in Figure 7a. For the 3-year observation period, MERRA-2 predicts an average accumulation rate of 20.0 cm w.e. a^{-1}, or 18% less than that from the snow board observations.

MAR version 3.12 is obtained from the Climate Center at Liege University (ftp://ftp.climato.be/fettweis/MARv3.12, last accessed: 8 February 2022). It has a 10-km resolution, daily output forced by the ERA5 reanalysis model. As with MERRA-2, MAR contains a dynamic ice-sheet surface and snow/firn layer model. MAR provides a daily estimate of SMB as a standard product. These are summed between snow board measurements to provide an estimate of the total change in SWE. As with MERRA-2, MAR predicts a substantially lower rate of accumulation than observed, averaging 18.8 cm w.e. a^{-1} and totaling 55.31 cm w.e., or 20% less than observed with the snow board.
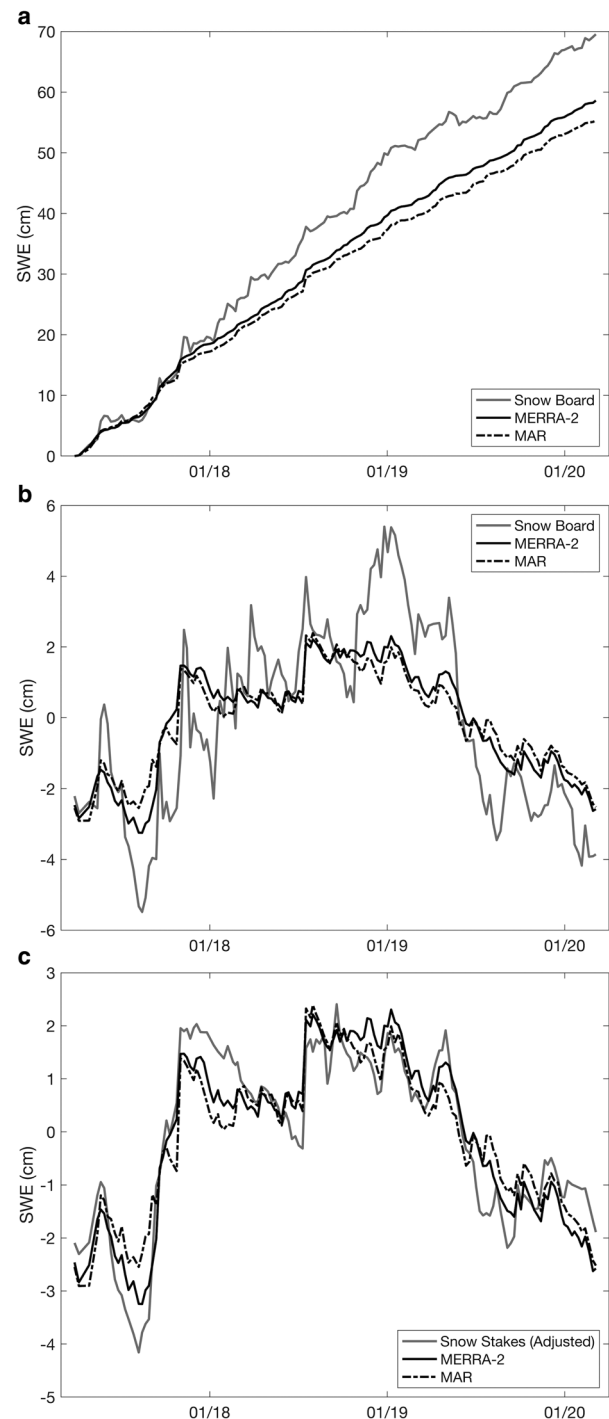
Removing the trend from both series (Fig. 7b) reveals that MERRA-2 and MAR capture much of the inter-annual and shorter-term variability, including the multiple single accumulation events, such as on 19 May and 6 November 2017, and 16 July 2018. Overall, MERRA-2 and MAR account for 75 and 70% of the variability in SWE. For MERRA-2, the RMS error in changes between measurements of 0.82 cm w.e. per 7 d, and 1.43 cm w.e. for the cumulative change in the detrended time series. For MAR, these are 0.85 cm w.e. per 7 d, and 1.67 cm for cumulative change in the detrended time series.

Spatial variability likely contributes to the differences between the snow board observations and reanalysis model estimates. The timing and magnitude of the differences in detrended series in Figure 7b appear similar to those between the snow board and snow stake snow depth changes plotted in Figure 5b. The detrended reanalysis model estimates and the cumulative change in SWE estimated from the snow stake average snow depth using a density of 0.3 g cm^{-3} are plotted in Figure 7c. These show a
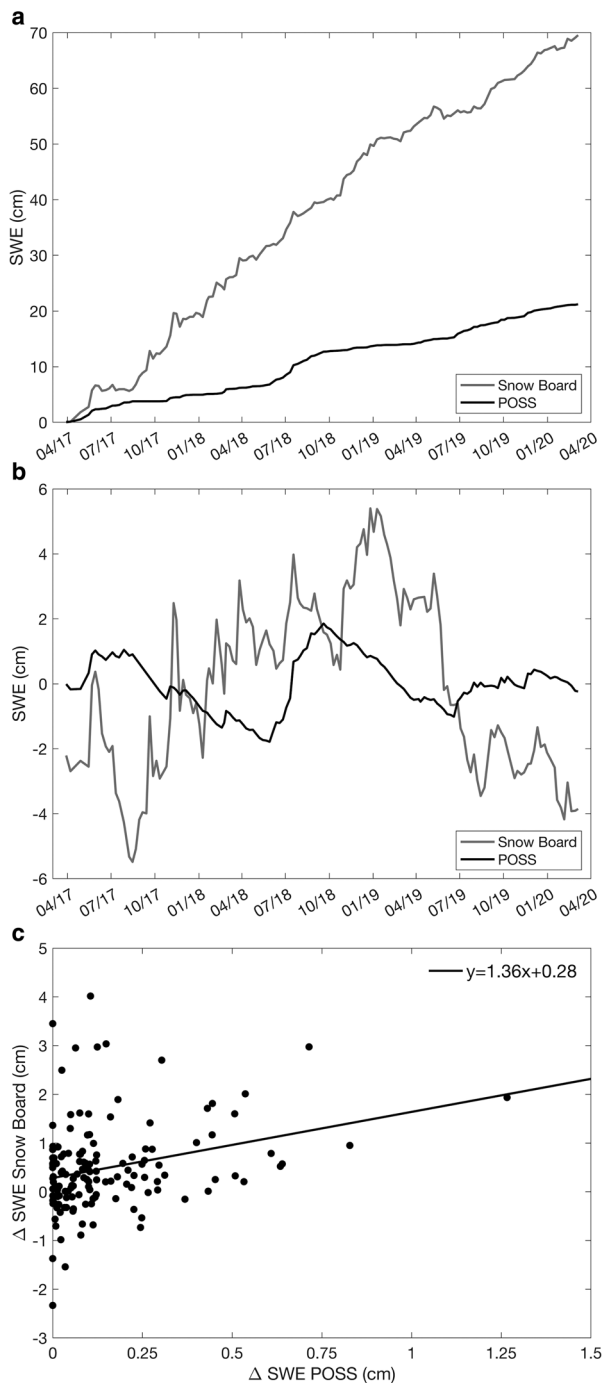
Fig. 6. (A) Cumulative SWE and (B) detrended cumulative SWE measured from the (black) POSS and (gray) snow board. (C) Scatter plot of changes in SWE from the POSS and snow board measured between snow board observations. Black curve is the line of best fit with the equation in legend.

Fig. 7. (A) Cumulative and (B) detrended SWE from (black curve) MERRA-2 and (dashes) MAR reanalysis model outputs and (gray) snow board observations. (C) Same as (B) but with gray curve as cumulative SWE estimated from the average of the snow stake network adjusted using a density of 0.3 g cm^{-3}.

closer agreement in sub-annual variability than the snow board observations, with the snow stakes accounting for 87 and 79% of the variability in MERRA-2 and MAR, respectively, and 7-d RMS errors of 0.30 and 0.33 cm w.e., respectively. This indicates that a significant portion of the sub-annual differences between snow board and reanalysis model estimates are due to spatial variability, which is better characterized by the spatially extensive snow stake network. However, the bias in average annual SWE accumulation rates is the same as with the snow board observations. Using the compaction rate of 15.12 cm a^{-1} estimated in Section 5 and a density of 0.3 g cm^{-3}, the snow stakes give an average annual SWE accumulation rate of 24.48 cm a^{-1}.

8. Conclusions

The first long-term, continuous and direct measurements of SWE accumulation on the Greenland ice sheet reveal increasing variability at shorter timescales. While the 3-year average annual accumulation is identical to the multi-decade average obtained from ice cores, year-to-year accumulation varied by over one-third of the average rate over the period of observation. This is larger than the maximum annual change of ~25% between 1974 and 1975 measured from a series of shallow cores spanning 1964–1987 around Summit Camp (Bolzan and Strobel, 1994). The reduction in accumulation rate was concurrent with exceptionally strong

and persistent anticyclonic conditions in the spring and summer of 2019 (Tedesco and Fettweis, 2020) that was reflected in extremely high-atmospheric pressure, lasting for several months at Summit Camp. While Summit Camp receives approximately half its snowfall from mixed-phase clouds originating from the southwest under anticyclonic conditions in the summer (Pettersen and others, 2018; McIlhattan and others, 2020), the 2019 event was anomalous in its pattern of sustained northerly flow, resulting in decreased snowfall in the interior ice sheet (Tedesco and Fettweis, 2020). This is apparent in the POSS measurements, which showed a greatly diminished seasonal peak in snowfall in summer of 2019 relative to the previous years. The fact that the 3-year mean is near the expected long-term average suggests anomalously high accumulation rates prior to 2019; the average accumulation rate was $28.33 \, \text{cm w.e. a}^{-1}$ from March 2017 to December 2018.

Consistent with Dibb and Fahnestock (2004), and despite multiple studies finding a seasonal cycle in snowfall (Bennartz and others, 2019), we find no evidence for a consistent annual cycle in accumulation at Summit Camp. Rather, the time series is dominated by the interannual variability described above and individual accumulation events throughout the year that could be due to snowfall and/or wind redistribution. Half of the accumulation was deposited in large events, mostly in 2017 and 2018, where the 7-d accumulation rate exceeded the 90th percentile and which individually were a substantial fraction (>10%) of the annual accumulation. Despite the co-occurrence of decreased accumulation and persistent high pressure in 2019, and the expectation for snowfall to correlate with southerly winds (Cullather and others, 2014; Pettersen and others, 2018; Gallagher and others, 2022), weekly accumulation rates do not significantly correlate with average surface wind direction or pressure. Conversely, cumulative mass losses, which exceed 1 cm w.e. in 7 d, are equivalent to nearly a quarter of the total mass gain. This loss is much larger than could be accounted for by sublimation (Box and Steffen, 2001) and, therefore, must be due to wind erosion and redistribution.

Local, short-term rates of wind erosion are lacking (Lenaerts and others, 2012), but several observations point to the importance of wind redistribution in controlling local accumulation. First is the lack of temporal correlation between accumulation and snowfall recorded by the POSS, which shows the expected late summer peak (Bennartz and others, 2019). This indicates another process regulates how a snowfall is accumulated. At weekly timescales, however, the POSS reveals that losses in SWE are larger during periods with lower cumulative snowfall, suggesting that snowfall does counter net erosion. Second, short-term differences in accumulation between the snow board and the snow stake network, as well as within the network itself, demonstrate significant spatial variability indicative of erosion and/or redistribution through transport in the air columns and/or drifting. Third, periods of greatest mass loss tended to follow large accumulation events, when wind erosion is expected to be fastest due to the low density of new snowfall (Lenaerts and others, 2012). Despite this evidence, there is no clear correlation between average wind speed and weekly accumulation, indicating a more complex relationship that is potentially dependent on surface winds, snow density, relative humidity and drifting, all operating on even shorter timescales than the snow board observations.

The density of the surface accumulation showed a variability of 10–20% on timescales ranging from weeks to years. Consistent with Fausto and others (2018), there is not a clear correlation with surface wind speed or temperature. On weekly timescales, due to these variations in density, changes in snow thickness account for only 60% of the change in mass. However, thickness changes become more representative of mass changes when differencing over longer periods of time, so that, assuming a standard surface density of $\sim 0.3 \, \text{g cm}^{-3}$, gives an estimate of mass

change within 5% after 1 year. Good agreement between snow depth change recorded at the snow board and the snow stake network average is achieved by accounting for compaction at a constant rate of $15.12 \, \text{cm a}^{-1}$, consistent with a previous estimate (Dibb and Fahnestock, 2004), indicating that variability at the snow board provides a representative measurement of the larger region on annual timescales and, conversely, mass accumulation can be estimated from the snow stake measurements at high relative accuracy at annual or longer timescales using these mean values for compaction rate and density.

Finally, the snow board measurements reveal substantial (18 and 20%) underestimates of accumulation by two prominent meteorological reanalysis models. This indicates a model bias toward too little snowfall in the Summit Camp region. Bennartz and others (2019) found a similar underestimate in snowfall accumulation in the ERA-Interim reanalysis model for Summit Camp when compared to that estimated from CloudSat cloud-profiling radar satellite observations calibrated with ground-based radar. They attributed this bias to the model not capturing shallow, more convective precipitation in the summer months. Additionally, using airborne snow-penetrating radar, Overly and others (2016) and Montgomery and others (2020) have detected underestimates of over 40% in reanalysis model snowfall estimates in western and southeastern Greenland, respectively. Therefore, this may be a widespread bias that could significantly bias mass-balance estimates; a 20% bias in the $700 \, \text{Gt a}^{-1}$ accumulation rate (Box and others, 2013) would represent $\sim$50% of the current rate of mass loss (IMBIE, 2020). However, with the multi-year trend removed, the reanalysis models capture much of the variability in accumulation on inter-annual and shorter timescales, suggesting that assessments of temporal variability using these models are more robust.

References

Alley R and 10 others (1993) Abrupt increase in Greenland snow accumulation at the end of the Younger Dryas event. *Nature* **362**(6420), 527–529. doi: 10.1038/362527a0

Bennartz R, Fell F, Pettersen C, Shupe MD and Schuettemeyer D (2019) Spatial and temporal variability of snowfall over Greenland from CloudSat observations. *Atmospheric Chemistry and Physics* **19**(12), 8101–8121. doi: 10.5194/acp-19-8101-2019

Berkelhammer M and 8 others (2016) Surface-atmosphere decoupling limits accumulation at summit, Greenland. *Science Advances* **2**(4), e1501704. doi: 10.1126/sciadv.1501704

Bolzan J and Strobel M (1994) Accumulation-rate variations around summit, Greenland. *Journal of Glaciology* **40**(134), 56–66. doi: 10.3189/S0022143000003798

Box JE and 10 others (2013) Greenland ice sheet mass balance reconstruction. Part I: net snow accumulation (1600–2009). *Journal of Climate* **26**(11), 3919–3934. doi: 10.1175/JCLI-D-12-00373.1

Box JE and Steffen K (2001) Sublimation on the Greenland ice sheet from automated weather station observations. *Journal of Geophysical Research-Atmospheres* **106**(D24), 33965–33981. doi: 10.1029/2001JD900219

Castellani BB, Shupe MD, Hudak DR and Sheppard BE (2015) The annual cycle of snowfall at summit, Greenland. *Journal of Geophysical Research-Atmospheres* **120**(13), 6654–6668. doi: 10.1002/2015JD023072

Cullather RI, Nowicki SMJ, Zhao B and Suarez MJ (2014) Evaluation of the surface representation of the Greenland ice sheet in a general circulation model. *Journal of Climate* **27**(13), 4835–4856. doi: 10.1175/JCLI-D-13-00635.1

Dibb J and Fahnestock M (2004) Snow accumulation, surface height change, and firn densification at summit, Greenland: insights from 2 years of in situ observation. *Journal of Geophysical Research-Atmospheres* **109**(D24), D24113. doi: 10.1029/2003JD004300

Fausto RS and 11 others (2018) A snow density dataset for improving surface boundary conditions in Greenland ice sheet firn modeling. *Frontiers in Earth Science* **6**, 51. doi: 10.3389/feart.2018.00051

Fettweis X and 6 others (2013) Estimating the Greenland ice sheet surface mass balance contribution to future sea level rise using the regional atmospheric climate model MAR. *The Cryosphere* **7**(2), 469–489. doi: 10.5194/tc-7-469-2013

Fettweis X and 40 others (2020) GrSMBMIP: intercomparison of the modelled 1980–2012 surface mass balance over the Greenland Ice sheet. *The Cryosphere* **14**(11), 3935–3958. doi: 10.5194/tc-14-3935-2020

Gallagher MR and Shupe MD, Chepfer H and L'Ecuyer T (2022) Relating snowfall observations to Greenland ice sheet mass changes: an atmospheric circulation perspective. *The Cryosphere* **2**, 435.

Gelaro R and 30 others (2017) The Modern-Era Retrospective Analysis for Research and Applications, Version 2 (MERRA-2). *Journal of Climate* **30**(14), 5419–5454. doi: 10.1175/JCLI-D-16-0758.1.

Global Modeling and Assimilation Office (GMAO) (2015) MERRA-2 tavg3_2d_glc_Nx: 2d,3-Hourly,Time-Averaged,Single-Level,Assimilation, Land Ice Surface Diagnostics V5.12.4, Greenbelt, MD, USA, Goddard Earth Sciences Data and Information Services Center (GES DISC) **2021** (Nov. 20).

Howat IM, de la Pena S, Desilets D and Womack G (2018) Autonomous ice sheet surface mass balance measurements from cosmic rays. *The Cryosphere* **12**(6), 2099–2108. doi: 10.5194/tc-12-2099-2018

IMBIE Team (2020) Mass balance of the Greenland ice sheet from 1992 to 2018. *Nature* **579**(7798), 233. doi: 10.1038/s41586-019-1855-2

Kuipers Munneke P and 10 others (2015) Elevation change of the Greenland ice sheet due to surface mass balance and firn processes, 1960–2014. *The Cryosphere*. 2009–2025, https://doi.org/10.5194/tc-9-2009-2015, 2015

Lenaerts JTM, Medley B, van den Broeke MR and Wouters B (2019) Observing and modeling ice sheet surface mass balance. *Reviews of Geophysics* **57**(2), 376–420. doi: 10.1029/2018RG000622

Lenaerts JTM, van den Broeke MR, van Angelen JH, van Meijgaard E and Dery SJ (2012) Drifting snow climate of the Greenland ice sheet: a study with a regional climate model. *The Cryosphere* **6**(4), 891–899. doi: 10.5194/tc-6-891-2012

McIlhattan EA, Pettersen C, Wood NB and L'Ecuyer TS (2020) Satellite observations of snowfall regimes over the Greenland ice sheet. *The Cryosphere* **14**(12), 4379–4404. doi: 10.5194/tc-14-4379-2020

Montgomery L, Koenig L, Lenaerts JTM and Kuipers Munneke P (2020) Accumulation rates (2009–2017) in southeast Greenland derived from airborne snow radar and comparison with regional climate models. *Annals of Glaciology* **61**(81), 225–233. doi: 10.1017/aog.2020.8

Overly TB, Hawley RL, Helm V, Morris EM and Chaudhary RN (2016) Greenland annual accumulation along the EGIG line, 1959–2004, from ASIRAS airborne radar and neutron-probe density measurements. *The Cryosphere* **10**(4), 1679–1694. doi: 10.5194/tc-10-1679-2016

Pettersen C and 5 others (2018) Precipitation regimes over central Greenland inferred from 5 years of ICECAPS observations. *Atmospheric Chemistry and Physics* **18**(7), 4715–4735. doi: 10.5194/acp-18-4715-2018

Sheppard BE and Joe PI (2008) Performance of the precipitation occurrence sensor system as a precipitation gauge. *Journal of Atmospheric and Oceanic Technology* **25**(2), 196–212. doi: 10.1175/2007JTECHA957.1

Sturm M and 5 others (2010) Estimating snow water equivalent using snow depth data and climate classes. *Journal of Hydrometeorology* **11**(6), 1380–1394. doi: 10.1175/2010JHM1202.1

Tedesco M and Fettweis X (2020) Unprecedented atmospheric conditions (1948–2019) drive the 2019 exceptional melting season over the Greenland ice sheet. *The Cryosphere* **14**(4), 1209–1223. doi: 10.5194/tc-14-1209-2020

Wayand NE and 5 others (2015) A meteorological and snow observational data set from Snoqualmie Pass (921 m), Washington Cascades, USA. *Water Resources Research* **51**(12), 10092–10103. doi: 10.1002/2015WR017773

Zwally HJ and Li J (2002) Seasonal and interannual variations of firn densification and ice-sheet surface elevation at the Greenland summit. *Journal of Glaciology* **48**, 199–207.